RSC Advances

ROYAL SOCIETY OF CHEMISTRY

www.rsc.org/advances

Graphical abstract

This work describes the synthesis and application of a novel magnetic metal-organic framework to preconcentrate trace amounts of heavy metals.

(a) A schematic diagram of Fe_3O_4 functionalization by ethylenediamine. **(b)** The schematic illustration of synthesized magnetic MOF nanocomposite.

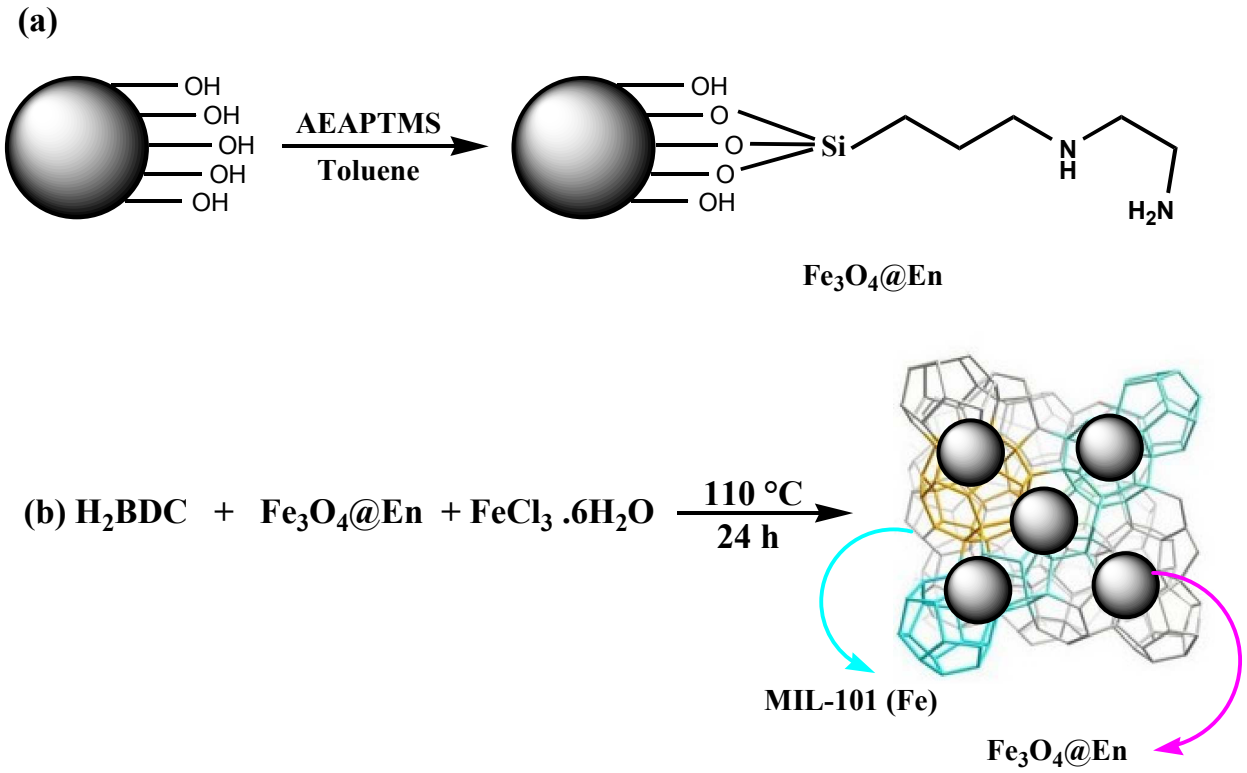

Solid phase extraction of heavy metal ions from agricultural samples with the aid of a novel functionalized magnetic metal-organic framework

Mirzaagha Babazadeh,[a,*] Rahim Hosseinzadeh Khanmiri[a], Jafar Abolhasani[a], Ebrahim Ghorbani-Kalhor[a], Akbar Hassanpour[b]

[a] *Department of Chemistry, Tabriz Branch, Islamic Azad University, Tabriz, Iran*

[b] *Department of Chemistry, Marand branch, Islamic Azad university, Marand, Iran*

Corresponding author: Fax: +98-491-2231616; Tel: +98 9143094107

E-mail: babazadeh@iaut.ac.ir (M. Babazadeh)

Abstract

This work describes the synthesis and application of a novel magnetic metal-organic framework (MOF) [(Fe_3O_4-ethylenediamine)/MIL-101(Fe)] to preconcentrate trace amounts of Cd(II), Pb(II), Zn(II) and Cr(III) ions and their determination by flame atomic absorption spectrometry. A Box-Behnken design was used to find the parameters affecting the preconcentration procedure through response surface methodology. Three variables including sorption time, amount of the magnetic sorbent, and sample pH were selected as affecting factors in sorption step, and four parameters including type, volume, concentration of the eluent, and elution time were selected in elution step for the optimization study. These values were 29 mg , 15 min, 6.1, EDTA+HNO_3, 4.2 mL, 0.7 mol L^{-1} EDTA in 0.07 mol L^{-1} HNO_3 solution, 17.0 min, for amount of the magnetic sorbent, sorption time, sample pH, type, volume, and concentration of the eluent, and elution time, respectively. The limits of detection (LOD) were 0.15, 0.8, 0.2 and 0.5 ng mL^{-1} for Cd(II), Pb(II), Zn(II) and Cr(III) ions, respectively. The relative standard deviations (RSD) of the method were less than 7.6% for five separate batch experiments in the determination of 30 μg L^{-1} of Cd(II), Pb(II), Zn(II) and Cr(III) ions. The sorption capacity of [(Fe_3O_4-ethylenediamine)/MIL-101(Fe)] was 155 mg g^{-1} for cadmium, 198 mg $g^{-1}$for lead, 164 for zinc and 173 mg g^{-1} for chromium. Finally, the magnetic MOF nanocomposite was successfully applied to rapidly extract trace amounts of heavy metal ions in agricultural samples.

***Keywords*:** Functionalized magnetic metal-organic framework nanocomposite; Heavy metal ions; Extraction; Agricultural samples.

1. Introduction

Heavy metal ions are toxic pollutants which exist in wastewaters and their presence concerns industries and environmental organizations all over the world. Most of these pollutants are very toxic and dangerous for human health. Thus determination of trace amounts of heavy metals is often a major task for the analytical chemists, as it is a good tool for the identification and monitoring of toxicants in environmental samples. Among heavy metals that exist in the environment, cadmium monitoring is very vital due to the fact that cadmium concentrations in the environment are increasing dramatically. [1,2] Cadmium exposure can be linked to diseases associated with aging such as osteoporosis, prostate, and pancreatic cancer. [3,4] Lead is one of the most toxic and hazardous elements in human health, because it can cause detrimental effect on metabolic processes of human beings. [5] It has been proven to be a carcinogenic agent. Zinc deficiency might lead to several disorders such as growth retardation, diarrhea, immunity depression, eye and skin lesions, malfunction of wound healing, and other skin diseases. [6] Cr(III) is an essential nutrient for humans. Cr(III) is effective on the mechanism of the glucose and cholesterol metabolism. In larger amounts and in different forms, chromium can be toxic and carcinogenic. [7] Though trace amounts of metals such as zinc are biotic for humans, the excess utilization can be harmful and toxic, so it should be used in the case of physiological needs. Thus the determination of trace amounts of heavy metals is one of the most important topics in analytical chemistry.

Various instrumental techniques, including electrothermal atomic absorption spectrometry (ETAAS),[8,9] inductively coupled plasma-optical emission spectrometry (ICP-OES),[10] flame atomic absorption spectrometry (FAAS),[11] inductively coupled plasma-mass spectrometry (ICP-MS),[12] and total reflection XRF-spectrometry[13] have been used for the determination of heavy

metals. Since the heavy metals concentration level in environmental samples is fairly low and the complexity of matrices is a main problem; thus preconcentration techniques are often required. [14] Different procedures such as: liquid-liquid extraction (LLE),[15] cloud point extraction,[16] chemical precipitation,[17] ion exchange,[18] and solid phase extraction (SPE) have been developed for the extraction and preconcentration of heavy metals in natural matrices. [19-21]

Among mentioned methods, the most commonly used technique for the preconcentration of heavy metal ions from environmental samples is solid phase extraction. Its common application is due to its simplicity, rapidity, minimal cost, and low consumption of reagents. [22] By the advent of SPE, various diverse sorbents have been utilized such as carbon nanotubes, [23,24] magnetic nanoparticles,[25,26] solid sulfur,[27] Cotton,[28] and modified porous materials. [29,30] Porous materials are defined as solids containing empty voids which can host other molecules. The fundamental features of these materials are their porosity, the ratio between total occupied and empty space, the (average) size of the pores and the surface area. Typical surface area values for the porous materials applied in technological processes range between 2000 and 8000 m^2 g^{-1}. [31] The most important applications of such materials are the storage of small molecules and filtering .The metal organic frameworks are defined as a nanocomposite material which can be consisted of either inorganic or organic materials. MOFs have shown high potential in gas storage, separation, chemical sensing, drug delivery, and heterogeneous catalysis applications. [32] In general, the flexible and highly porous structure of MOFs allows guest species such as metal ions to diffuse into their bulk structure. The shape and size of the pores lead to selectivity over the guests that may be adsorbed. These features make MOFs an ideal sorbent in solid phase extraction of heavy metals. However, there is little information about MOFs as an adsorbent. [33]

In this work, for the first time a magnetic metal organic framework immobilized with Fe_3O_4-ethylenediamine (Fe_3O_4@En) has been utilized as a novel adsorbent for the fast separation and the preconcentration of Cd(II), Pb(II), Zn(II) and Cr(III) ions in various matrixes. The magnetic sorbent was characterized by, X-ray diffraction (XRD), Fourier transform infrared spectroscopy (FT-IR), scanning electron microscopy (SEM) and elemental analysis. The magnetic property of the sorbent causes a rapid and easy separation of the new solid phase from the solution. The presence of ethylenediamine in the sorbent helps the new solid phase to show selectivity towards these heavy metals. Also MOF cavities can increase the surface area and sorption capacity of this new sorbent. A Box-Behnken design was used in order to find the optimum conditions of the method through response surface methodology. Finally, the sorbent was used for the preconcentration and determination of Cd(II), Pb(II), Zn(II) and Cr(III) ions in different real samples and satisfactory results were obtained.

2. Experimental

2.1. Reagents and solutions

All reagents of analytical grade ($FeCl_2$, $FeCl_3.6H_2O$, $3H_2O$, HCl, HNO_3, K_2SO_4, NaOH, KCl, thiourea (TU), EDTA, N-(2-Aminoethyl)-3-(aminopropyl)trimethoxysilane (AEAPTMS), benzene-1,4-dicarboxylic acid (H_2BDC), toluene, triethylamine (TEA), tetrahydrofuran (THF), dimethylformamide (DMF) ethanol, dimethylformamide, methanol and acetone) were purchased from Merck (Darmstadt, Germany) or from Fluka (Seelze, Germany) and were used without further purification. Standard solutions of 1000 mg L^{-1} of Cd(II), Pb(II), Zn(II) and Cr(III) were purchased from Merck. All solutions were prepared using double distilled water.

119

120 *2.2. Instrumentation*

121 An AA-680 Shimadzu (Kyoto, Japan) flame atomic absorption spectrometer with a deuterium
122 background corrector was used for the determination of Cd(II), Pb(II), Zn(II) and Cr(III) ions.
123 Cadmium, lead, zinc and chromium hollow cathode lamps (HCL) were used as the radiation
124 sources with wavelengths of 228.8, 283.3, 213.9 and 357.9 nm, respectively. All measurements
125 were carried out in an air/acetylene flame. The pH of the solutions were measured at 25 ± 1 ºC
126 with a digital WTW Metrohm 827 Ion analyzer (Herisau, Switzerland) equipped with a
127 combined glass-calomelelectrode. IR spectra were recorded by a Bruker IFS-66 FT-IR
128 Spectrophotometer. High-angle X-ray diffraction patterns were obtained using a Philips-PW 17C
129 diffractometer with Cu Kα radiation (Philips PW, The Netherlands). CHN analysis was
130 performed on a Thermo Finnigan Flash EA112 elemental analyzer (Okehampton, UK). Scanning
131 electron microscopy (SEM) was performed by gently distributing the sample powder on the
132 stainless steel stubs, using an SEM (KYKY-3200, Beijing, China) instrument. Transmission
133 electron microscopy (TEM) analysis was performed by a LEO 912AB electron microscope (Leo
134 Ltd., Germany).

135

136 *2.3. Preparation of standard solution*

137 Standard Stock solutions (1000 mg L^{-1}) of K^+, Na^+, Ag^+, Ca(II), Mg(II), Fe(III), Cu(II), Mn(II),
138 Al(III), Ni(II), Hg(II), Co(II), and AsO_4^{3-} were prepared in a 2% (v/v) HNO_3 solution. The
139 working standard solutions were prepared by diluting an appropriate amount of the stock
140 solution with double distilled water. All of these solutions were stored in ambient temperature.

141

142 *2.4. Synthesis of magnetic metal-organic framework nanocomposite*

143 *2.4.1. Synthesis of Fe_3O_4@ethylenediamine*

144 Fe_3O_4 nanoparticles were synthesized according to previously reported procedure. [25] It was then
145 modified with AEAPTMS. In a typical reaction, 1.5 g of Fe_3O_4 was suspended in 50 mL
146 toluene, and the mixture was stirred for 45 min. Then AEAPTMS (1.5 mL) was added to the
147 mixture and it was refluxed for 12 h under nitrogen atmosphere. [34] Thereafter the solid was
148 removed from the solvents by magnetic separation washed with methanol and acetone and then
149 dried at room temperature (Fig. 1a). The synthesis of ethylenediamine-functionalized Fe_3O_4
150 (Fe_3O_4@En) was characterized by IR spectroscopy, high-angle X-ray diffraction, scanning
151 electron microscopy, and elemental analysis.

152

153 *2.4.2. Synthesis of MIL-101(Fe) metal-organic framework*

154 MIL-101(Fe) metal-organic framework was synthesized according to the previously reported
155 procedure. [35] A solution containing 1.03 g of H_2BDC and 3.25 g of $FeCl_3.6H_2O$ in 100 mL of
156 DMF was sonicated for 15 min and then under vigorous stirring. The mixture was transferred
157 into an autoclave and it was heated at 110 ^oC for 24 h. The obtained powder was recovered by
158 centrifugation, washed once with water and then with ethanol four times to remove impurities.
159 Afterwards, it was dried under vacuum at 100 °C for 16 h and kept under dry nitrogen until
160 further use. The synthesized MOF was characterized by IR spectroscopy, CHN analysis, SEM,
161 and XRD.

162

163 *2.4.3. Synthesis of magnetic metal-organic framework nanocomposite*

Magnetic MOF nanocomposite was synthesized according to the following procedure (Fig. 1b). First 0.5 g Fe_3O_4@En was dispersed in a solution containing 3.38 g of $FeCl_3.6H_2O$ and 40 mL DMF by sonicating for 15 min. Then this mixture was added to another solution containing 1.03 g of H_2BDC in 50 mL DMF and sonicated for 10 min. Thereafter the mixture was transferred into an autoclave and it was heated at 110 ^oC for 24 h. Finally, the product was isolated from the supernatant solution by magnetic decantation and washed with water (50 mL) and hot ethanol (15 mL × 5). Magnetic sorbent was characterized by IR spectroscopy, CHN analysis, SEM, and XRD.

2.5. Sorption and elution step

Extraction of heavy metal ions from aqueous solutions was investigated by batch analysis. Sorptions were performed in test tubes containing 25 μg of Cd(II), Pb(II), Zn(II) and Cr(III) ions in 50 mL of double distilled water. According to a preliminary experimental design, the pH of the solutions were adjusted by the drop wise addition of 1.0 mol L^{-1} ammonia and 1.0 mol L^{-1} hydrochloric acid. Then magnetic sorbent was added into the solutions. After that, the mixture was stirred for an appropriate time to extract these heavy metal ions from the solution completely. Finally, the test tubes were exposed to a strong magnet (15 cm × 12 cm × 5 cm, 1.4 T), where permanent magnet in the wall caused the particles to aggregate on one side of the test tube. The adsorbed amounts of Cd(II), Pb(II), Zn(II) and Cr(III) ions were determined using FAAS due to the concentration change for these ions in solution after sorption. The instrument response was periodically checked with known Cd(II), Pb(II), Zn(II) and Cr(III) ions standard solutions. Extraction percentage for each ion was calculated using the following equation:

$$\textbf{Extraction}\% = \frac{\mathbf{C_A - C_B}}{\mathbf{C_A}} \times \mathbf{100}$$

where C_A and C_B are initial and final concentrations (mg L^{-1}) of each ion in the solution, respectively. In the elution step, 4.2 mL 0.7 mol L^{-1} EDTA in 0.07 mol L^{-1} HNO_3 solution as an eluent was added to the magnetic sorbent and shaken. This mixture was again exposed to a strong magnet and the clear solution of eluent, containing the eluted heavy metal ions was introduced to FAAS in order to determine the amount of each ion.

2.6. Real sample pretreatment

2.6.1. Agricultural samples

The agricultural samples including leek, fenugreek, parsley, radish, radish leaves, beetroot leaves, garden cress, basil and coriander were collected from Tehran growing areas (Shahriyar-Tehran). Cleaned polyethylene bags were applied to supply the samples according to their type. After washing samples with distilled water, they were dried at 100 °C for 2 days. For the preparation of spiked samples, 1.0 mL of the standard working solution was added to 1.0 g of each sample. They were then allowed to stand at room temperature for the evaporation of the solvent; therefore, the equilibration between the analytes and the agricultural products was achieved. After grinding the dry samples (spiked or non-spiked), microwave-assisted acid digestion was carried out by adding 2 mL of distilled water, 4 mL of nitric acid 65%, and 2 mL of hydrogen peroxide 33% (w/v) to 0.5 g of each sample. The reactors were then subjected to the microwave program as following: [36] 2.5 min at room temperature, 6 min at 140 °C, 5 min at 200

°C in power of 550 W. After acid digestion was completed, the acid digests were diluted up to 25 mL with distilled water and kept in a refrigerator before magnetic solid phase extraction.

2.6.3. Reference material

The concentration of the heavy metal ions was determined at optimum conditions in standard reference materials (NIST SRM 1573a tomato leaves and NIST SRM 1515 apple leaves). The standard material was digested according to the mentioned procedure for agricultural samples. The pH of the solution was adjusted to 6.1 for the separation and preconcentration of Cd(II), Pb(II), Zn(II), and Cr(III) ions form the solution. Finally, the preconcentration procedure mentioned above was applied to the resulted solutions.

2.7. Experimental design methodology

In order to fully understand the effect of the experimental variables that can significantly affect the extraction procedure, individual factors must be considered along with nonlinear effects and interaction terms. The chemometric approach has a rational experimental design, which allows simultaneous variation of all experimental factors, reducing the required time and number of trials which results in the reduction the overall required costs. The Box-Behnken design (BBD) is probably the most widely used experimental design applied for fitting a second-order response surface. This cubic design is characterized by a set of points lying at the midpoint of each edge of a multidimensional cube and center point replicates whereas the 'missing corners' help the experimenter to avoid using the combined factor extremes. This property prevents a potential loss of data in those cases. [37]

In this study the StatGraphics plus 5.1 package was used for the analysis of the experimental design data and calculating the predicted responses.

3. Results and discussion

3.1. Characterization studies

3.1.1. FT-IR spectra and elemental analysis

The FT-IR spectra of MOF, and magnetic nanocomposite were recorded using KBr pellet method. The advent of the absorption peaks due to Fe-O (585 cm^{-1}), Si-O-Si (1039 cm^{-1}), C-H aliphatic (2933 and 2885 cm^{-1}), and N-H (3441 cm^{-1}) confirmed the immobilization of MOF by Fe_3O_4@En. Moreover, elemental analysis showed the presence of 3.2% N in the structure of the magnetic nanocomposite. This data indicates that Fe_3O_4@En had been sufficiently immobilized in the structure of magnetic nanocomposite (C: 23.5%, H: 1.6%, N: 3.2%).

3.1.2. Scanning electron microscopy

To investigate the surface morphology of the Fe_3O_4@En NPs, MOF and magnetic nanocomposite, the samples were characterized by TEM or SEM (Fig. 2). As it is illustrated in Fig. 2a, the spherical structure of Fe_3O_4 NPs was approximately preserved after modification with AEAPTMS. In this figure, two regions with different electron densities can be distinguished which confirms the formation of the core-shell structure: [38] an electron dense region which corresponds to Fe_3O_4 cores with a uniform size of about 10-30 nm and a less dense and more translucent region surrounding these cores that is AEAPTMS coating shell with a thickness of about 10-15 nm. Furthermore, the TEM micrograph confirmed that the Fe_3O_4@En NPs are nano-sized with an average particle size of 30 nm. The crystals of original MIL-101 (Fe) sample have

a smooth surface with an average size of 200 nm (Fig. 2b). However, surface of the magnetic nanocomposite tends to be rougher after Fe_3O_4@En immobilization (Fig. 2c). It was apparent that the modified Fe_3O_4 NPs were linked to the external surface of the MIL-101 crystals.

3.1.3. X-ray diffraction analysis

For further study, MOF and magnetic nanocomposite were characterized by XRD. All of the diffraction peaks of MIL-101 (Fe) can be seen in Fig. 1S (Electronic Supplementary Data) before modification. For magnetic nanocomposite, modification of MIL-101 (Fe) with Fe_3O_4@En resulted in a loss of crystalline order in the framework. It is evidenced by a significant decrease in diffraction intensities (Fig. 3b), which is due to the partial decomposition of the crystalline MIL-101 (Fe). [33,35] The advent of five characteristic peaks for Fe_3O_4 in the XRD parent of magnetic MOF and also the presence of three characteristic peaks for MIL-101 (Fe) revealed that this hybrid material was composed of Fe_3O_4@En and MIL-101 (Fe).

3.2. Optimization of the preconcentration procedure

3.2.1. Sorption step

The optimization step for the sorption of metal ions on the magnetic nanocomposite was carried out using Box-Behnken design (BBD). Variables affecting the extraction efficiency were chosen: pH, amount of the magnetic nanocomposite, and extraction time. Other parameters involved in the extraction were kept constant, especially the concentration of heavy metal ions (0.5 mg L^{-1}). This design permitted the responses to be modeled by fitting a second-order polynomial, which can be expressed as the following equation:

$$Y = \beta_0 + \beta_1 x_1 + \beta_2 x_2 + \beta_3 x_3 + \beta_{12} x_1 x_2 + \beta_{13} x_1 x_3 + \beta_{23} x_2 x_3 + \beta_{11} x_1^2 + \beta_{22} x_2^2 + \beta_{33} x_{13}^2$$

where, x_1, x_2, and x_3 are the independent variables, β_0 is an intercept, β_1- β_{33} are the regression coefficients, and Y is the response (removal% or recovery%). The number of experiments (N) is defined by the expression below:

$$N = 2K\,(K - 1) + C_o$$

where K is the number of variables and C_o is the number of center points. [39] In this study, K and C_o were set at 3 and 6 respectively, which meant that 18 experiments had to be done. The levels of the factors are listed in Table 1. The analysis of variance (ANOVA) results producing the Pareto chart of main and interaction effects which are shown in Fig. 3a. The standard effect was estimated for computing the t-statistic for each effect. The vertical line on the plot shows statistically significant effects. The bar extracting beyond the line corresponds to the effects that are statistically significant at 95% confidence level. [40-44] Furthermore, the positive or negative sign (corresponding to a colored or colorless response) can enhance or reduce the extraction efficiency, respectively, while increasing from the lowest to the highest level set for the specific factor. According to Pareto chart the pH of the solution has the most significant positive effect on the extraction efficiency. The sorption of heavy metal ions increases as the pH increases. In acidic solution, sorption is very low. This observation is due to the protonation of the magnetic nanocomposite active sites especially N atoms of ethylenediamine. As the pH increases, the protonation of these active sites decreases and the condition becomes more favorable for complex formation and adsorption of heavy metal ions to the magnetic nanocomposite. At pH > 6.1 the extraction efficiencies of target ions decreased due to the formation of insoluble hydroxide forms of metals. To avoid the precipitation of metal ions at higher pH values, pH 6.1

was selected as optimum. The response surface methodology (RSM) and two-dimensional contour plot (Fig. 3b) was applied to analysis simultaneous effects of sorption time and pH variables on the response. The sorption efficiency of heavy metal ions increased along with the increase in pH while the extraction time had a non-significant positive effect on the extraction of these ions. Sorption time and amount of the magnetic nanocomposite both showed positive and significant effect on the extraction efficiency. According to the overall results of the optimization study, the following experimental conditions were chosen: pH, 6.1; sorption time, 15 min; amount of the magnetic nanocomposite, 29 mg.

3.2.2. Selection of eluent

In this work several eluents including HCl, HNO_3, K_2SO_4, NaOH, KCl, thiourea, EDTA solution and mixture of them were examined as the desorption solvent. Other factors were kept constant during the optimization (pH, 6.1; sorption time, 15 min; amount of the magnetic nanocomposite, 29 mg; eluent volume, 7.0 mL; elution time, 20 min). Results showed that HNO_3 containing EDTA can recover the target ions. In the next step the effect eluent volume and its concentration as well as elution time were optimized.

3.2.3. Elution step

Three factors were studied in elution step using experimental design: eluent volume (mL), elution time (min), HNO_3 concentration (mol L^{-1}) and EDTA concentration (mol L^{-1}). In these conditions, a response surface design could be done without previously performing a screening design. The BBD was chosen because it requires the least number of experiments (29 run). The data obtained were evaluated by ANOVA. The results of the experimental design were evaluated

318 at 5% of significance and analyzed by standardized Pareto chart (Fig. 4a). Based on BBD, all
319 parameters showed positive and significant effect on the recovery of target ions. These
320 observations are most possibly due to increased protonation of the hetero atoms of the sorbent as
321 the concentration of the eluent increases as well as coordination of heavy metal ions with EDTA
322 and also fast kinetics of elution process is of great importance. As Fig. 4a shows, EDTA
323 concentration has the greatest influence on the extraction recovery. The RSM and two-
324 dimensional contour plot (Fig. 4b) were applied to analyze simultaneous effects of the elution
325 time and eluent volume on the responses. The extraction efficiency of the heavy metal ions
326 increased along with an increase in the eluent volume and also elution time. According to the
327 overall results of the optimization study, the following experimental conditions were chosen as
328 the optimized ones: eluent volume, 4.2 mL; elution time, 17 min; and eluent concentration, 0.70
329 mol L^{-1} EDTA in 0.07 mol L^{-1} HNO_3 solution.
330
331 *3.3. Effect of breakthrough volume*
332 In the analysis of real samples, the sample volume is one of the important parameters affecting
333 the preconcentration factor. The breakthrough volume of sample solutions was investigated by
334 dissolving 1 mg of each Cd(II), Pb(II), Zn(II) and Cr(III) ion in 100, 250, 500, 750, 1000, 1250
335 and 1500 mL of distilled water. Then the SPE protocol was performed. The results demonstrated
336 that the dilution effect was not significant for sample volumes of 1000 mL for each ion on the
337 magnetic nanocomposite. Thus, the new sorbent enabling an enrichment factor of 238 was
338 obtained for Cd(II), Pb(II), Zn(II) and Cr(III) ions.
339
340 *3.4. Effect of the potentially interfering ions*

To investigate the effect of the potentially interfering ions found in natural samples, various metal ions were added to 250 mL of a solution containing 10 μg of each ion. The degree of tolerance for potentially interfering ions is presented in Table 1S (Electronic Supplementary Data). From the tolerance results, it can be seen that even high levels of the potentially interfering ions has no impact on the preconcentration of Cd(II), Pb(II), Zn(II) and Cr(III) ions at pH 6.1. So the method could be applied to determine these heavy metal ions in complicated matrix samples.

3.5. Sorption capacity study and reusability of the sorbent

In order to investigate the sorption capacity of the magnetic nanocomposite a standard solution containing 7.0 mg L^{-1} of Cd(II), Pb(II), Zn(II) and Cr(III) ions was used. In order to evaluate the maximum sorption capacity, the initial and equilibrium amounts of heavy metal ions were determined by FAAS. The maximum sorption capacity is defined as the total amount of heavy metal ions sorbed per gram of the magnetic nanocomposite. The obtained capacities of the magnetic nanocomposite were found to be 155, 198, 164, and 173 mg g^{-1} for Cd(II), Pb(II), Zn(II) and Cr(III) ions, respectively.

The reusability of magnetic nanocomposite was tested by assessing the change in the recoveries of the analytes through several sorption-elution cycles under the opted conditions. The results revealed that the synthesized nanosorbent could be reused up to 12 times.

3.6. Analytical performance of the method

Under the optimal conditions, calibration curves were constructed for the determination of Cd(II), Pb(II), Zn(II) and Cr(III) ions, according to the mentioned procedure. Linearity was

within the range of 0.5-100 ng mL^{-1} for Cd(II), 2.5-250 ng mL^{-1} for Pb(II), 0.6-120 ng mL^{-1} for Zn(II) and 1.5-150 ng mL^{-1} for Cr(III) in initial solution. The correlation of determination (r^2) was 0.9975 for Cd(II), 0.9964 for Pb(II), 0.9938 for Zn(II) and 0.9955 for Cr(III) ions. The limit of detection is defined as LOD = $3S_b/m$, where S_b is the standard deviation of 10 replicate blank signals and m is the slope of the calibration curve after preconcentration. For a sample volume of 1000 mL, it was found to be 0.15 ng mL^{-1} for Cd(II), 0.8 ng mL^{-1} for Pb(II), 0.2 ng mL^{-1} for Zn(II), and 0.5 ng mL^{-1} for Cr(III) ions. The precision of the method for a standard solution containing 30 ng mL^{-1} of heavy metal ions (n = 5) was evaluated as the relative standard deviation (RSD%) and was found to be 7.6, 4.9, 6.8 and 5.5%, for Cd(II), Pb(II), Zn(II) and Cr(III) ions respectively.

3.7. Validation of the method

The concentrations of Cd(II), Pb(II), Zn(II) and Cr(III) ions obtained by current method were compared to the exact concentration of these ions in the standard reference materials. For this reason, the concentration of the heavy metal ions was determined at optimum conditions in standard reference materials (NIST SRM 1573a tomato leaves and NIST SRM 1515 apple leaves). As it can be seen in Table 2, good correlation was achieved between the estimated content by the present method and reference materials. Therefore, the magnetic nanocomposite can be used as a reliable solid phase for the extraction and determination of Cd(II), Pb(II), Zn(II) and Cr(III) ions in agricultural samples.

3.8. Determination of target ions in agricultural samples

Since natural samples have complex matrices, non-specific background absorption is always caused by interfering species of the sample matrix. To reduce this undesirable effect, the magnetic nanocomposite was applied for the selective extraction of Cd(II), Pb(II), Zn(II) and Cr(III) ions in pH 6.1. Table 3 shows the Cd(II), Pb(II), Zn(II) and Cr(III) ions recovery in various agricultural samples which in all cases, were almost quantitative.

Conclusion

A simple, fast, reproducible, and selective solid-phase extraction procedure, a novel magnetic metal-organic framework nanocomposite, for determining of cadmium, zinc, chromium and lead ions has been developed. In comparison with other solid-phases, the magnetic nanocomposite has the advantages of high enrichment capacity, low limit of detection, and high enrichment factor (Table 2S, Electronic Supplementary Data). Other advantages of this method are: (1) low time-consumption due to the magnetically-assisted separation of the adsorbent and higher surface area; therefore, satisfactory results can be achieved by using fewer amounts of the adsorbents. Due to the relatively high preconcentration factor, trace amounts of heavy metal at ng mL^{-1} levels in high-volume samples can be quantified by the magnetic nanocomposite.

Acknowledgements

The authors would like to thank Tabriz Branch, Islamic Azad University, Tabriz, Iran, for the financial support of this research.

409

410

411

412

413

414

415

416 **References**

417 [1] U. Farooq, M.A. Khan, M. Athar, J.A. Kozinski*, Chem. Eng. J.*, 2011, **171**, 400-410.

418 [2] J.N. Bianchin, E. Martendal, R. Mior, V.N. Alves, C.S.T. Araújo, N.M.M. Coelho, E.
419 Carasek, *Talanta*, 2009, **78**, 333-336.

420 [3] N.M. Kalariya, B. Nair, D.K. Kalariya. N.K. Wills, F.J.G.M.V. Kuijk, *Toxicol. Let.*, 2010,
421 **198**, 56-62.

422 [4] M. Gharehbaghi, M. Davudabadi Farahani, F. Shemirani, *Anal. Methods*, 2014, DOI:
423 10.1039/C4AY01531B

424 [5] A.A. Asgharinezhad, H. Ebrahimzadeh, M. Rezvani, N. Shekari, M. Loni, *Food Addit.*
425 *Contam.: Part A*, 2014, **31**, 1196-1204.

426 [6] H. Scherz, E. Kirchhoff, *J. Food Comp. Anal.*, 2006, **19**, 420-433.

427 [7] Z. Bahadir, V.N. Bulut, D. Ozdes, C. Duran, H. Bekta, M. Soylak, *J. Ind. Eng. Chem.*, 2014,
428 **20**, 1030-1034.

[8] D. Bohrer, P. Cícero do Nascimento, M. Guterres, T. Trevisan, E. Seibert, *Analyst*, 1999, **124**, 1345-1350.

[9] Y.-H. Sung, S.-D. Huang, *Anal. Chim. Acta*, 2003, **495**, 165-176.

[10] E.L. Silva, P. dos Santos Roldan, M.F. Giné, *J. Hazard. Mater.*, 2009, **171**, 1133-1138.

[11] C. Duran, H.B. Senturk, L. Elci, M. Soylak, M. Tufekci, *J. Hazard. Mater.*, 2009, **162**, 292-299.

[12] J. Yin, Z. Jiang, G. Chang, B. Hu, *Anal. Chim. Acta*, 2005, **540**, 333-339.

[13] B. Zawisza, R. Sitko, *Spectrochim. Acta B Atomic Spect.*, 2007, **62**, 1147-1152.

[14] P. Bruno, M. Caselli, G. Gennaro, P. Ielpo, T. Ladisa, C.M. Placentino, *Chromatographia*, 2006, **64**, 537-542.

[15] S. Abe, K. Fuji, T. Sono, *Anal. Chim. Acta*, 1994, **293**, 325-330.

[16] J. Chen, K.C. Teo, *Anal. Chim. Acta*, 2011, **450**, 215-222.

[17] M.M. Matlock, B.S. Howerton, D.A. Atwood, *Water Res.*, 2002, **36**, 4757-4764.

[18] M.C. Yebra-Biurrun, A. Bermejo-Barrera, M.P. Bermejo-Barrera, M.C. Barciela-Alonso, *Anal. Chim. Acta*, 1995, **303**, 341-345.

[19] M. Rezvani, A.A. Asgharinezhad, H. Ebrahimzadeh, N. Shekari, *Microchim. Acta*, 2014, DOI 1 0.1007/s00604-014-1262-1.

[20] A. Duran, M. Tuzen, M. Soylak, *J. Hazard. Mater.*, 2009, **169**, 466-471.

[21] M. Tuzen, M. Soylak, L. Elci, *Anal. Chim. Acta*, 2005, **548**, 101-108.

448 [22] M. Tuzen, K.O. Saygi, M. Soylak, *J. Hazard. Mater.*, 2008, **156**, 591-595.

449 [23] A.A. ALOthman, M. Habila, E. Yilmaz, M. Soylak, *Microchim. Acta*, 2012, **177**, 397-403.

450 [24] M. Taghizadeh, A.A. Asgharinezhad, N. Samkhaniany, A. Tadjarodi, A. Abbaszadeh, M.
451 Pooladi, *Microchim Acta*, 2014, **181**, 597-605.

452 [25] A.A. Asgharinezhad, N. Mollazadeh, H. Ebrahimzadeh, F. Mirbabaei, N. Shekari, *J.*
453 *Chromatogr. A*, 2014, 1338, 1-8.

454 [26] A.A. Asgharinezhad, H. Ebrahimzadeh, F. Mirbabaei, N. Mollazadeh, N. Shekari, *Anal.*
455 *Chim. Acta*, 2014, 844, 80-89.

456 [27] H. Parham, N. Pourreza, N. Rahbar, *J. Hazard. Mater.*, 2009, **163**, 588-592.

457 [28] M. Faraji, Y. Yamini, S. Shariati, *J. Hazard. Mater.*, 2009, **166**, 1383-1388.

458 [29] M.R. Sohrabi, Z. Matbouie, A.A. Asgharinezhad, A. Dehghani, *Microchim. Acta*, 2013,
459 **180**, 589-597.

460 [30] M. Taghizadeh, A.A. Asgharinezhad, M. Pooladi, M. Barzin, A. Abbaszadeh, A. Tadjarodi,
461 *Microchim. Acta*, 2013, **180**, 1073-1084.

462 [31] H.K. Chae, D.Y. Siberio-Perez, J. Kim, Y. Go, M. Eddaoudi, A.J. Matzger, M. O'Keeffe,
463 O.M. Yaghi, *Nature*, 2004, **427**, 523-527.

464 [32] O. Shekhah, J. Liu, R.A. Fischer, C. Wöll, *Chem. Soc. Rev.*, 2011, **40**, 1081-1106.

465 [33] F. Ke, L.-G. Qiu, Y.-P. Yuan, F.-M. Peng, X. Jiang, A.-J. Xie, Y.-H. Shen, J.-F. Zhu, *J.*
466 *Hazard. Mater.,* 2011, **196**, 36-43.

[34] A.S.M. Chong, X.S. Zhao, *J. Phys. Chem. B*, 2003, **107**, 12650-12657.

[35] S. Bauer, C. Serre, T. Devic, P. Horcajada, J. Marrot, G. Fe´rey, N. Stock, *Inorg. Chem.,* 2008, **47**, 7568-7576.

[36] A.B. Yilmaz, *Environ. Res.* 2003, **92**, 277-281.

[37] G.E.P. Box, N.R. Draper, *Empirical Model Building and Response Surfaces*, John Wiley and Sons, New York, 1987.

[38] H. Helmi, R. Helmi, N. Shahtahmassebi, M.R. Roknabadi, N. Ghows, *Nanomed. J.,* 2014, **1**, 71-78.

[39] F. Kamarei, H. Ebrahimzadeh, A.A. Asgharinezhad, *J. Sep. Sci.*, 2011, **34**, 2719-2725.

[40] StatGraphics Plus 5.1 for Windows, Statistical Graphic Crop., online manuals, 2001.

[41] H. Ebrahimzadeh, N. Shekari, Z. Saharkhiz, A.A. Asgharinezhad, *Talanta*, 2012, **94**, 77-83.

[42] H. Ebrahimzadeh, N. Mollazadeh, A.A. Asgharinezhad, N. Shekari, F. Mirbabaei, *J. Sep. Sci.*, 2013, **36**, 3783-3790.

[43] L. Adlnasab, H. Ebrahimzadeh, A.A. Asgharinezhad, M. Nasiri Aghdam, A. Dehghani, S. Esmaeilpour, *Food Anal. Methods*, 2014, **7**, 616-628.

[44] V. Amani, S. Roshan, A.A. Asgharinezhad, E. Najafi, H. Abedi, N. Tavassoli, H.R. Lotfi Zadeh Zhad, *Anal. Methods*, 2011, **3**, 2261-2267.

Figure captions

Fig. 1: (a) A schematic diagram of Fe_3O_4 functionalization by En. (b) The schematic illustration of synthesized magnetic MOF-En nanocomposite.

Fig. 2: (a) The TEM image of Fe_3O_4@En, the SEM images of (b) MOF, and (c) magnetic MOF nanocomposite.

Fig. 3: (a) Pareto chart of the main effects in the BBD (uptake step). AA, BB and CC are the quadratic effects of sample pH, the uptake time and the nanosorbent amount, respectively. AB, AC and BC are the interaction effects between sample pH and the uptake time; pH and the nanosorbent amount and the uptake time and the nanosorbent amount, respectively. (b) RSM and two-dimensional contour plot obtained by plotting pH *vs.* uptake time using the BBD.

Fig. 4: (a) Pareto chart of the main effects in the BBD (elution step). AA, BB, CC and DD are the quadratic effects of HNO_3 concentration, EDTA concentration, eluent volume and elution time, respectively. AB, AC, AD, BC, BD and CD are the interaction effects between HNO_3 concentration and EDTA concentration; HNO_3 concentration and eluent volume, HNO_3 concentration and elution time, EDTA concentration and eluent volume, EDTA concentration and elution time, and eluent volume and elution time respectively. (b) RSM and two-dimensional contour plot obtained by plotting eluent volume *vs.* elution time using the BBD.

Fig. 1

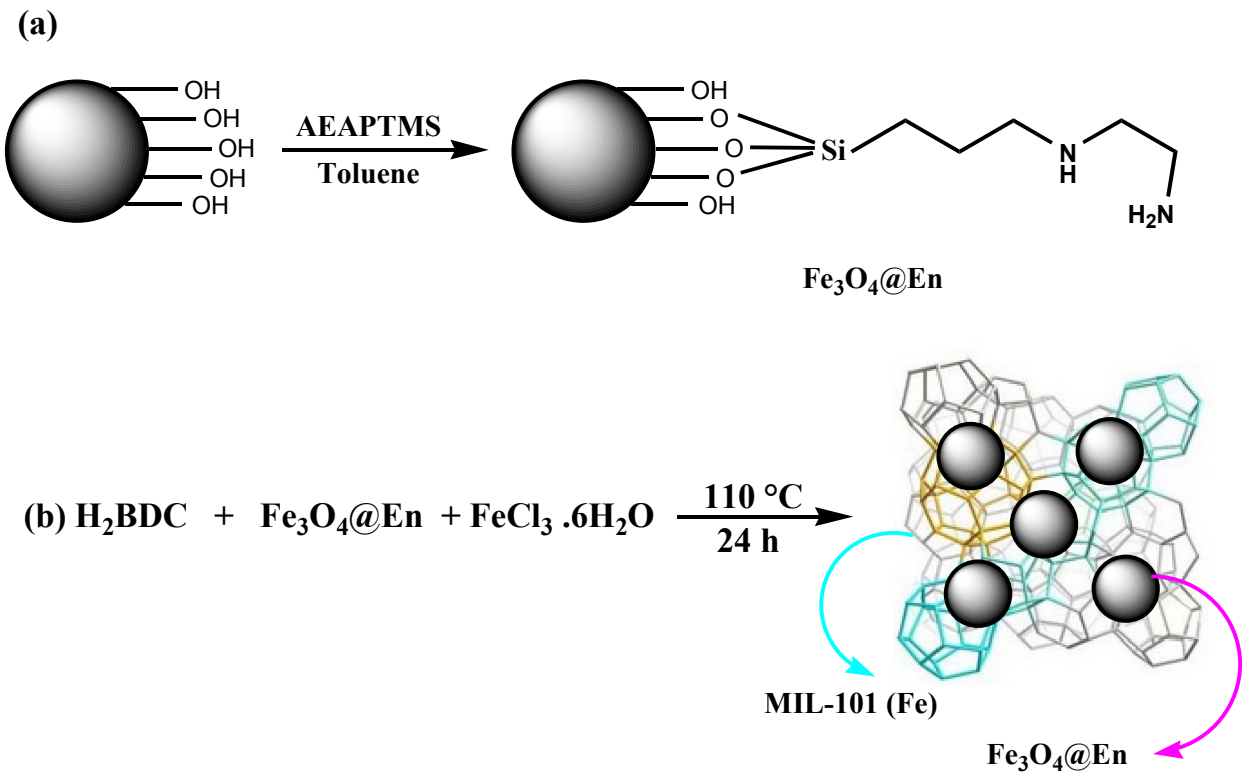

Fig. 2

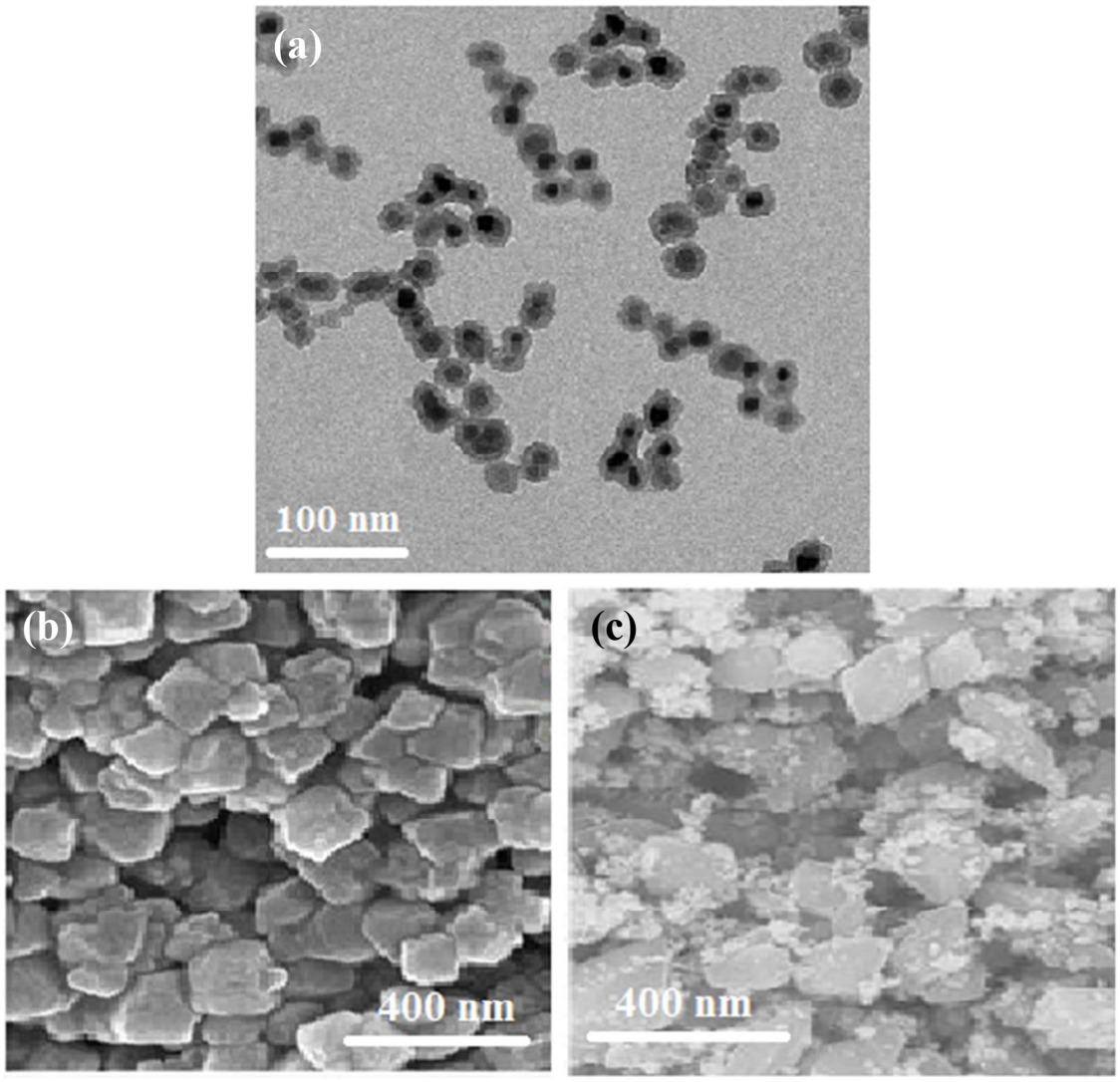

Fig. 3

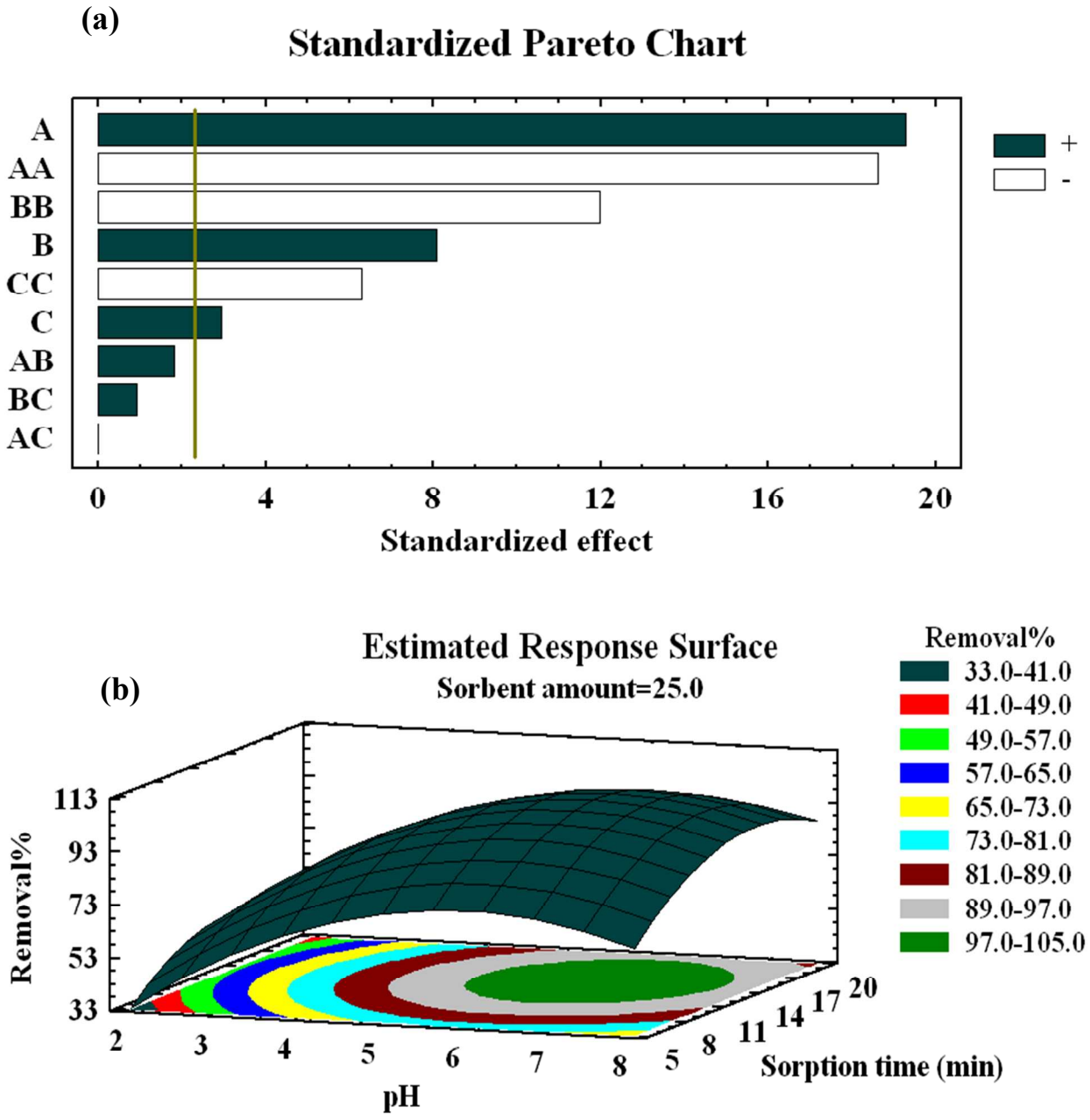

Fig. 4

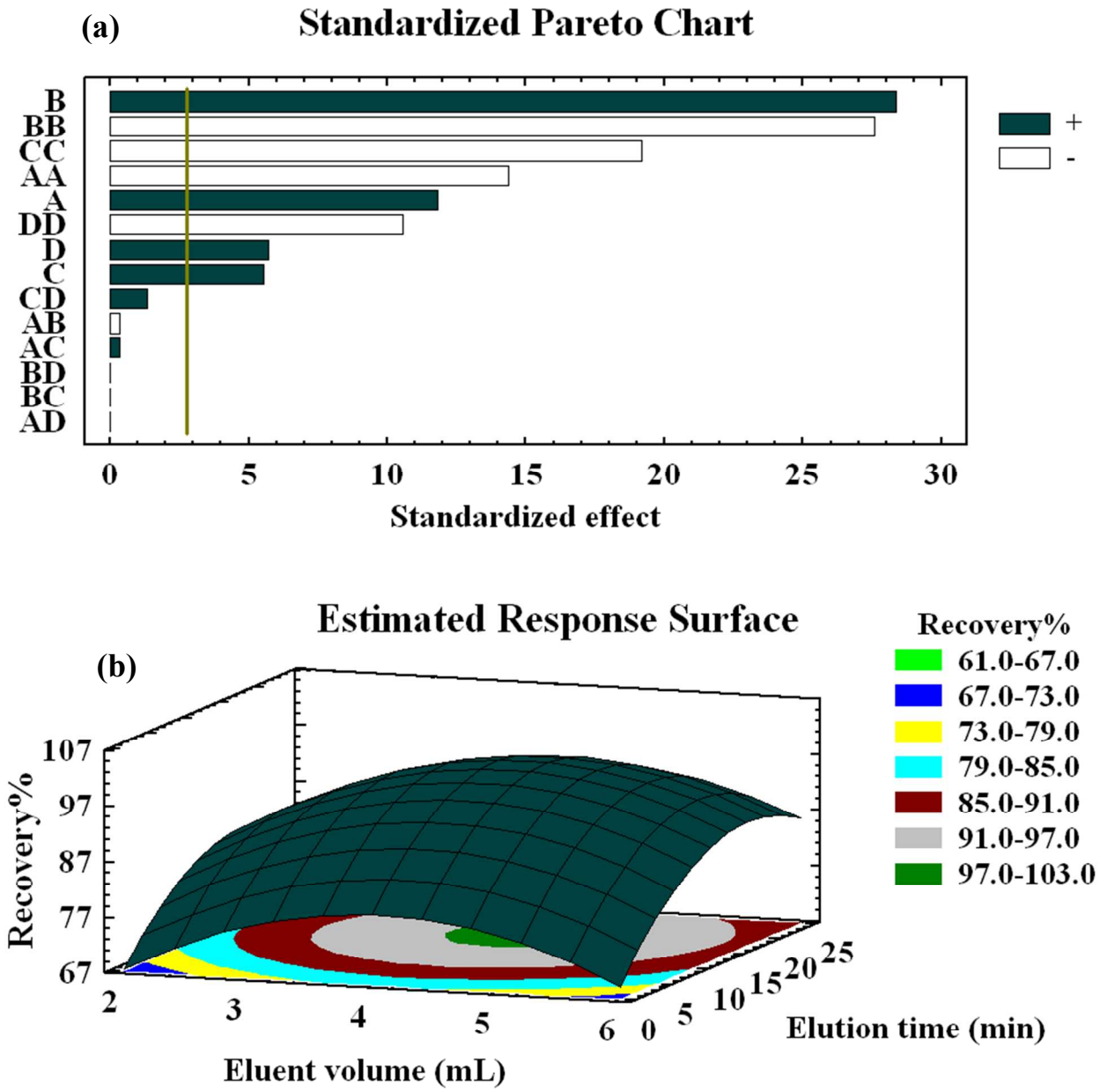

Table1
Experimental variables and levels of the Box Behnken design (BBD).

		Level		
		Lower	Central	Upper
Sorption step	A: pH	2.0	5.0	8.0
	B: Uptake time (min)	5.0	12.5	20.0
	C: Nanocomposite amount (mg)	5	25	45
Elution step	A: HNO_3 concentration (mol L^{-1})	0.01	0.055	0.1
	B: EDTA concentration (mol L^{-1})	0	0.5	1.0
	C: Eluent volume (mL)	2.0	4.0	6.0
	D: Elution time (min)	10.0	15.0	25.0

Table 2
Determination of heavy metal ion recovery in certified reference materials.

Sample	Concentration ($\mu g\ g^{-1}$)			Relative error%
	Element	Certified	Found	
NIST SRM 1515 apple leaves	Cd	0.013	0.012	-7.7
	Zn	12.5	12.0	-4.0
	Pb	0.47	0.51	8.5
	Cr	-	BDL	-
SRM 1570a spinach leaves	Cd	1.52	1.56	2.6
	Zn	-	BDL	-
	Pb	-	BDL	-
	Cr	1.99	2.06	3.5

BDL: below the detection limit.

Table 3
Determination of heavy metal ions in agricultural samples.

Sample	Element	Real sample (μg g^{-1})	Added (μg g^{-1})	Found (μg g^{-1})	Recovery (%)
Leek	Cd	4.5	5.0	9.0	90.0
	Pb	9.4	10.0	19.2	98.0
	Zn	267	250	526	104
	Cr	4.4	5.0	9.6	104
Fenugreek	Cd	3.2	5.0	8.0	96.0
	Pb	41.0	50.0	92.1	102
	Zn	105	100	196	91.0
	Cr	4.2	5.0	9.6	108
Garden cress	Cd	1.7	2.0	3.6	95.0
	Pb	59.1	50.0	104	89.8
	Zn	192	200	380	94.0
	Cr	3.3	5.0	8.1	96.0
Radish	Cd	3.2	5.0	8.1	98.0
	Pb	52.6	50.0	104	103
	Zn	102	100	204	102
	Cr	4.5	5.0	9.2	94.0
Radish leaves	Cd	2.2	5.0	7.3	102
	Pb	4.7	5.0	9.5	96.0
	Zn	203	200	398	97.5
	Cr	6.4	10.0	15.5	91.0
Beetroot leaves	Cd	1.4	5.0	6.5	102
	Pb	9.0	10.0	18.6	96.0
	Zn	152	150	296	96.0
	Cr	7.4	10.0	18.0	106
Basil	Cd	1.0	2.0	2.9	95.0
	Pb	7.2	10.0	16.8	96.0
	Zn	145	150	284	92.7
	Cr	8.5	10.0	18.6	101
Coriander	Cd	1.9	2.0	4.1	110
	Pb	16.5	10.0	27.1	106
	Zn	169	150	300	87.3
	Cr	5.6	5.0	10.0	88.0
Parsley	Cd	2.8	5.0	7.5	94.0
	Pb	18.3	20.0	38.4	106
	Zn	200	200	393	96.5
	Cr	5.6	10.0	15.3	97.0